Proceedings Paper:

McAree, O. and Veres, S.M. (2017) Lateral control of vehicle platoons with on-board sensing and Inter-Vehicle Communication. In: 2016 European Control Conference (ECC). 2016 European Control Conference (ECC), 29 Jun - 01 Jul 2016, Aalborg, Denmark. IEEE. ISBN: 978-1-5090-2591-6.

https://doi.org/10.1109/ECC.2016.7810660

Lateral control of vehicle platoons with on-board sensing and Inter-Vehicle Communication

Owen McAree and Sandor M. Veres

Department of Automatic Control and Systems Engineering
University of Sheffield
Sheffield, UK
Email: {o.mcaree, s.veres}@sheffield.ac.uk

***Abstract*—This paper presents a lateral control strategy for a platoon of vehicles which utilises only data which can realistically be measured by each vehicle, augmented with Inter-Vehicle Communication (IVC). The control problem resembles those which exist for longitudinal control and this introduces the challenge of estimating a vehicles lateral position and velocity when direct measurement is not possible (due to lane markings being obscured by a preceding vehicle). It is shown that the associated robust controller, which we propose, exhibits string stability in the presence of sensor and actuation delays and a high fidelity simulation is conducted to verify this.**

I. Introduction

Modern motorways have become increasingly congested leading to increased environmental and economic impacts in addition to an unpleasant driving experience. Combine this with the inevitable boredom which can set in on long journeys (and the serious accidents this lack of attention can cause [1]) and it is little surprise that advances in technology are being used to mitigate these problems. One such technology is *platooning*, in which a number of vehicles autonomously follow a leader (which may be manually or autonomously driven) enabling greater road utilisation and fuel efficiency with a reduction in accidents.

Platooning has been of interest to vehicle manufacturers for over 20 years, with significant theoretical developments in addition to full scale demonstrations [2]–[6]. It has been demonstrated that if the inter-vehicle spacing can be reduced to below $8m$, a significant fuel saving of up to 15% can be realised [7]. Reducing the spacing to these values, however, causes a problem for the lateral (steering) control of a platooning vehicle.

Early attempts at platooning systems solved the lateral control problem by placing magnetic markers in the road surface, which were detected by the platooning vehicles, allowing them to determine their lateral position [8], [2]. This solution, however, requires a significant infrastructure investment which is likely to outweigh many of the benefits. For platoons to be economically viable, they must be able to operate within the existing infrastructure, without modification [9].

To achieve this it is necessary to re-purpose the Lane Departure Warning System (LDWS) camera [10] to detect the preceding vehicle, rather than lane markings, and use this information to calculate lateral position. In order to do this, we need some additional information from both the preceding vehicle and platoon leader to be transmitted via an Inter-Vehicle Communication (IVC) system [11]. Whilst this may initially seem prohibitive, it has been shown that to achieve stable performance of longitudinal control at low spacing values IVC is also required [12] and this has not caused a significant barrier to development.

The stability of a platoon controller is determined not only by the stability of individual vehicles but also by the *string stability* of the entire system. It has been demonstrated that in order to achieve string stability for lateral control, IVC is necessary [13] and some work has been conducted which does not require a direct estimate of lateral position [14]. This paper presents a novel approach which first attempts to estimate the lateral position of the vehicle from sensor and IVC information, then control this value using similar techniques to those developed for longitudinal control.

The next section details the estimation of lateral position from sensor and IVC information and comments on the robustness of the approach to both measurement error and delays. Section III then details the controller design and verifies its string stability under nominal operation and in the presence of delays. In Section IV we present results from a high-fidelity simulation which verify string stability on both straight and curved roads and robustness in the presence of delays. Finally, we conclude with some observations and discussion of further research.

II. Lateral position estimation

Outside of a platoon, a vehicle fitted with LDWS can detect lane markings with a forward looking camera to determine its lateral position on the road. As inter-vehicle distances are reduced in a platooning scenario this becomes very difficult as the preceding vehicle will largely obscure the lane markings. The same camera system, however, can be used to measure a vehicle's relative position to the preceding vehicle, allowing the lateral position to be estimated.

Here we consider the estimation problem for the (ith) vehicle in a string of $i = 1 \dots n$ vehicles of a platoon. It is

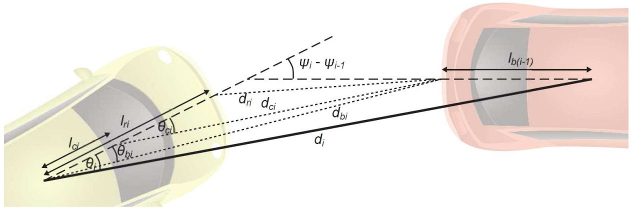

Fig. 1. Calculation of azimuth and distance from sensor data. l_{ci} and l_{ri} are the distances of the camera and radar from the ith vehicle's centre of mass. $l_{b(i-1)}$ is the distance of the rear bumper from the $(i-1)$th vehicle's centre of mass. d_{ri} is the distance from the radar to the rear bumper. (d_{ci}, θ_{ci}), (d_{bi}, θ_{bi}) and (d_i, θ_i) are the distanced and angles between the camera and rear bumper, centre of mass and rear bumper and centre of masses respectively. $\psi_i - \psi_{i-1}$ is the heading difference.

first assumed that the preceding ($(i-1)$th) vehicle is aware of its own lateral position (y_{i-1}) and it is able to transmit this to the ith vehicle via an IVC system. This is not an unreasonable assumption as the lead vehicle will be able to detect lane markings with LDWS and subsequent vehicles will transmit their estimates, obtained from this technique. The camera system of the ith vehicle can detect the azimuth of the centre of the rear bumper preceding vehicle (θ_{ci}) and a radar system (likely present for longitudinal control) can detect the inter-vehicle distance (d_{ri}), see schematic of the geometry in Fig. 1. These on-board sensors are not typically mounted at the centre of mass, neither do they detect the centre of mass of the vehicle ahead, it is therefore necessary to calculate the true azimuth (θ_i) and distance (d_i).

A. Calculation of azimuth and distance from sensor data

We shall assume that the sensors detecting the vehicle azimuth and distance are placed a distance l_{ci} and l_{ri} ahead of the centre of mass respectively. Both sensors are assumed to be on the vehicle centreline and able to detect the centre of rear bumper of the car ahead. Fig. 1 illustrates the geometry of the problem which requires knowledge of the heading difference between the two vehicles ($\delta\psi_i = \psi_i - \psi_{i-1}$) to be estimated. This may be obtainable from an additional sensor, but most likely will require the vehicle ahead to transmit its heading via an IVC system.

Calculating θ_i and d_i requires the calculation of some intermediate values, namely d_{ci}, θ_{bi} and d_{bi}, the distance from camera to rear bumper and the angle and distance from the centre of mass to the rear bumper respectively. It also requires knowledge of the distance from the centre of mass of the $(i-1)$th vehicle to its rear bumper ($l_{b(i-1)}$), which may either be assumed or transmitted by the vehicle. From Fig. 1 we can see that

$$d_{ci} = (l_{ri} - l_{ci})\cos\theta_{ci} + \sqrt{d_{ri}^2 - (l_{ri} - l_{ci})^2 \sin^2\theta_{ci}} \quad (1)$$

$$\theta_{bi} = \tan^{-1}\left(\frac{d_{ci}\sin\theta_{ci}}{d_{ci}\cos\theta_{ci} + l_{ci}}\right) \quad (2)$$

$$d_{bi} = \sqrt{d_{ci}^2 + l_{ci}^2 + 2d_{ci}l_{ci}\cos\theta_{bi}} \quad (3)$$

From these values we can determine

$$d_i = \sqrt{d_{bi}^2 + l_{bi}^2 + 2d_{bi}l_{b(i-1)}\cos(\delta\psi_i - \theta_{bi})} \quad (4)$$

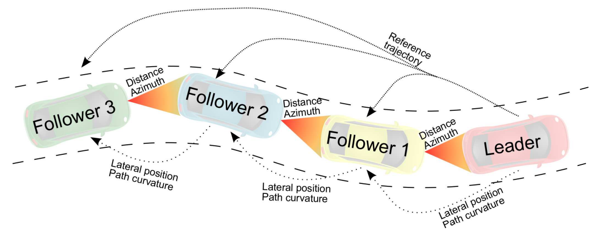

Fig. 2. IVC between leader and follower vehicles

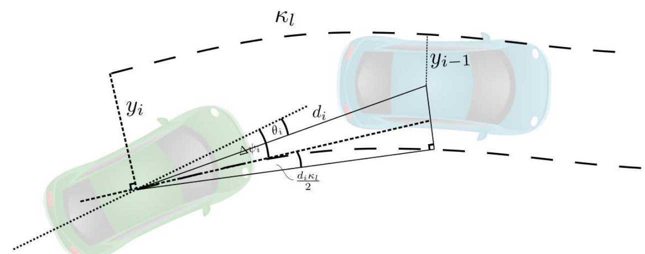

Fig. 3. Lateral position estimation. y_i and y_{i-1} are the lateral positions of the ego and preceding vehicles respectively. (d_i, θ_i) are the distance and angle between the centre of masses of the two vehicles, calculated from Fig. 1. κ_l is the reference curvature. $\Delta\psi_i$ is the heading deviation of the ith vehicle from the reference.

$$\theta_i = \delta\psi_i - \tan^{-1}\left(\frac{d_{bi}\sin(\delta\psi_i - \theta_{bi})}{d_{bi}\cos(\delta\psi_i - \theta_{bi}) + l_{b(i-1)}}\right) \quad (5)$$

B. Buffering of reference trajectory

In addition to information about the preceding vehicle, it is necessary to know a reference trajectory. The leader measures both the curvature (κ_l) and heading (ψ_l) of road and transmits this information to all follower vehicles. Each vehicle must buffer this data and choose an appropriate reference point based on their following distance behind the leader. Delaying the use of transmitted data in this way reduces the sensitivity of follower vehicles to communication delays from the leader, provided these delays remain significantly lower than the time gap between the vehicles. Fig. 2 illustrates the IVC requirements of both the leader and follower vehicles.

C. Lateral position calculation

Fig. 3 illustrates the geometry of lateral position estimation. To simplify the calculation it is assumed that κ_l is small, and approximately constant between the $(i-1)$th and ith vehicle. Therefore

$$y_i = y_{i-1} + d_i \sin(\Delta\psi_i - \theta_i + \frac{d_i\kappa_l}{2}) \quad (6)$$

where $\Delta\psi_i = \psi_i - \psi_l$, the difference between the ith vehicles heading and that of the reference trajectory.

D. Robustness to sensor errors

It is clear that if θ_{ci} and d_{ri} are subject to measurement error then these will propagate through (1)-(6), resulting in an erroneous lateral position estimate. To assess the effect of this a 1.8×10^6 run Monte-Carlo simulation was performed with range and azimuth measurement sampled from the Gaussian distributions

$$d_{ri} = \mathcal{N}(\hat{d}_{ri}, (1cm)^2) \quad (7)$$

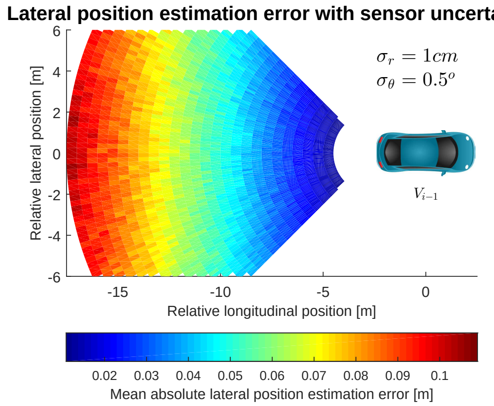

Fig. 4. Lateral position estimation error subject to sensor uncertainty. Coloured contours represent mean absolute error for the ith vehicles sensors located behind a preceding vehicle (V_{i-1})

$$\theta_{ci} = \mathcal{N}(\hat{\theta}_{ci}, (0.5^o)^2) \tag{8}$$

where $\hat{d}_{ri}$ and $\hat{\theta}_{ci}$ are the truth values. It was assumed that the radar and camera sensors were co-located (i.e. $l_{ri} = l_{ci}$) on the front bumper of the follower vehicle. Additionally, it is assumed that both vehicles were travelling on a straight, parallel trajectory (i.e. $\kappa_l = 0$, $\delta\psi_i = 0$ and $\Delta\psi_i = 0$), as this is the most common condition when platooning. Performance analysis on non-straight trajectories is given later in Section IV.

Fig. 4 illustrates the mean absolute lateral position error for a range of sensor positions behind a preceding vehicle. It is apparent that the error is strongly correlated with separation distance whilst exhibiting little correlation to azimuth. This is a desirable situation as the technique described above is only required when following distances are too small to permit the use of LDWS. Robustness to azimuth, however, is needed in order to assure adequate controller performance during lateral manoeuvres.

E. Robustness to sensor and communication delay

In addition to erroneous measurements, there is likely to be a delay in both the sensors and the communication from the preceding vehicle. To assess the affect of these delays on the lateral position estimation, a simulation environment which includes sensor and communication models (detailed in Section IV) was used to run a small (36 run) Monte Carlo study.

Fig. 5 illustrates the lateral position estimation error for a platoon of 9 follower vehicles, subject to sensor and communication delays up to $100ms$. It is clear that these delays compound the error along the length of the platoon, with communications delay being particularly significant. It is anticipated that the minimum achievable sensor and communication delays will impose a strict maximum platoon length in order to ensure the last vehicle is capable of sufficiently accurate lateral position estimation.

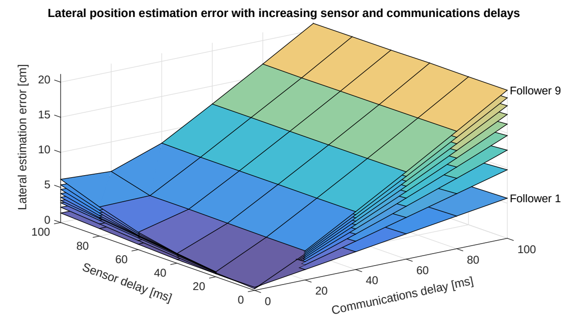

Fig. 5. Lateral position estimation error subject to sensor and communication delays

III. Lateral Control Design

A. Controller derivation

The lateral controller is derived in the same way as that for longitudinal control [12]. First, we define a sliding surface

$$S_i = \Delta\dot{y}_i + a\Delta y_i + b(\dot{y}_i - \dot{y}_l) + c(y_i - y_l) \tag{9}$$

where y_l is the lateral deviation of the leader from the reference trajectory and $\Delta y_i = y_i - y_{i-1}$ is obtained from (6).

To ensure sliding takes place, we set $\dot{S} = -\lambda S$, yielding

$$\begin{aligned} \Delta\ddot{y}_i + a\Delta\dot{y}_i + b(\ddot{y}_i - \ddot{y}_l) + c(\dot{y}_i - \dot{y}_l) = \\ -\lambda\Delta\dot{y}_i - a\lambda\Delta y_i - b\lambda(\dot{y}_i - \dot{y}_l) - c\lambda(y_i - y_l) \end{aligned} \tag{10}$$

To simplify subsequent derivation we assume that in calculating $\Delta\ddot{y}_i$ we can ignore the angular terms in (6) as changes in the heading and curvature between the ith and $(i-1)$th vehicles are small, therefore we can write

$$\Delta\ddot{y}_i = \ddot{y}_i - \ddot{y}_{i-1} \tag{11}$$

Substituting (11) in to (10) and rearranging for $\ddot{y}_i$ gives

$$\begin{aligned} \ddot{y}_i = \frac{1}{b+1}(\ddot{y}_{i-1} + b\ddot{y}_l - (a+\lambda)\Delta\dot{y}_i - a\lambda\Delta y_i - \\ (b\lambda + c)(\dot{y}_i - \dot{y}_l) - c\lambda(y_i - y_l)) \end{aligned} \tag{12}$$

For small heading deviations, $\ddot{y}_i$ is equivalent the lateral acceleration of the vehicle, which can be controlled through steering input via an inner control loop. It is more conventional however, to control the path curvature as this can be more easily measured [15]. Therefore, using the relationship $\ddot{y} = \kappa V^2$, where V is the forward speed of the platoon, we obtain

$$\begin{aligned} \kappa_i = \frac{\kappa_{i-1} + b\kappa_l}{b+1} - \frac{1}{(b+1)V^2}((a+\lambda)\Delta\dot{y}_i + \\ a\lambda\Delta y_i + (b\lambda + c)(\dot{y}_i + \dot{y}_l) + c\lambda(y_i - y_l))) \end{aligned} \tag{13}$$

where κ_i is now the desired path curvature of the ith vehicle. κ_{i-1} is the path curvature of the $(i-1)$th vehicle which must be sent to the ith vehicle via an IVC system. y_i is obtained from (6), which can be numerically differentiated to give $\dot{y}_i$.

B. Nominal string stability

String stability refers to the damping out of disturbances along the length of the platoon and is obtained when the following conditions are met [12]

$$|H_i(j\omega)| \leq 1 \tag{14}$$

$$h_i(t) > 0 \tag{15}$$

where $H_i(s) = \Delta y_i(s)/\Delta y_{i-1}(s)$ is the error propagation transfer function of the ith vehicle and $h_i(t)$ is its impulse response.

To determine $H_i(s)$ we first calculate $S_i - S_{i-1}$ from (9)

$$\begin{aligned} S_i - S_{i-1} = \Delta\dot{y}_i - \Delta\dot{y}_{i-1} + a(\Delta y_i - \Delta y_{i-1}) \\ b(\dot{y}_i - \dot{y}_{i-1}) + c(y_i - y_{i-1}) \end{aligned} \tag{16}$$

Assuming (11) holds for lower order terms we obtain

$$S_i - S_{i-1} = (1+b)\Delta\dot{y}_i - \Delta\dot{y}_{i-1} + (a+c)\Delta y_i - b\Delta y_{i-1} \tag{17}$$

Taking the Laplace transform of (17) and noting that sliding drives the left hand side to zero gives

$$H_i(s) = \frac{\Delta y_i(s)}{\Delta y_{i-1}(s)} = \frac{s+a}{(b+1)s + (a+c)} \tag{18}$$

Therefore

$$|H_i(j\omega)|^2 = \frac{\omega^2 + a^2}{(b+1)^2\omega^2 + (a+c)^2} \tag{19}$$

which satisfies (14) provided $a, b, c > 0$

The impulse response of (18) is given by

$$h_i(t) = \mathcal{L}^{-1}(H_i(s)) = \frac{ab - c}{(b+1)^2} e^{-\frac{a+c}{b+1}t} \tag{20}$$

which satisfies (15) provided

$$ab > c \tag{21}$$

C. String stability subject to unmodelled sensor and actuation delays

The previous section determined conditions for string stability without taking in to account the delays present in the sensing and dynamics of the system. It is important to assure that the string stability of the controller is robust to these delays. We can model delays as a first order filter applied to the lateral acceleration command given by (12) [16]

$$\tau\dddot{y}'_i + \ddot{y}'_i = \ddot{y}_i \tag{22}$$

where τ is the delay and $\ddot{y}'_i$ is the actual, delayed, lateral acceleration of the vehicle subject to the command $\ddot{y}_i$. Substituting (22) in to (12) and conducting a similar analysis to that above yields a new transfer function

$$H'_i(s) = \frac{1}{b+1} \frac{s^2 + (a+\lambda)s + a\lambda}{\tau s^3 + s^2 + (\lambda + \frac{a+c}{b+1})s + \lambda\frac{a+c}{b+1}} \tag{23}$$

Calculating the inequality (14) for (23) yields the polynomial

$$A\omega^6 + B\omega^4 + C\omega^2 + D \geq 0 \tag{24}$$

where

$$A = (b+1)^2\tau^2$$

Fig. 6. The Open Race Car Simulator (TORCS) [17]

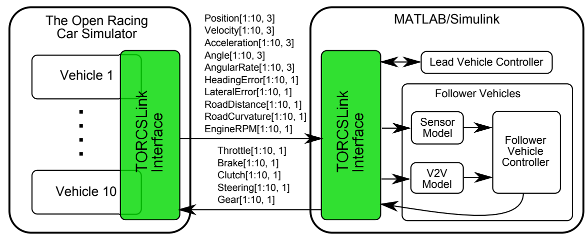

Fig. 7. Interface between TORCS and MATLAB/Simulink [18]

$$B = b(b+2) - 2\tau(b+1)^2(\lambda + \frac{a+c}{b+1})$$

$$C = 2ac + b\lambda^2(b+2) + c^2$$

$$D = \lambda^2(2ac + c^2)$$

It is clear that, subject to the conditions from the previous section, A, C and D are always positive. B is positive if the following inequality is satisfied

$$\tau \leq \frac{b(b+2)}{2(b+1)^2(\lambda + \frac{a+c}{b+1})} \tag{25}$$

This imposes an upper limit on the delays that can be tolerated whilst still maintaining lateral string stability.

IV. Simulation Results

A. Set up

To test the lateral platoon controller derived in the previous section a high fidelity simulation was performed using The Open Race Car Simulator (TORCS) [17], Fig. 6. An interface was written to link TORCS with MATLAB/Simulink [18], enabling the controller to be developed and tested quickly, Fig. 7.

Vehicle data is exported from TORCS at 50Hz and represents the truth data for each vehicle. The controllers for the follower vehicles are not fed directly with this truth data, but instead are provided with the outputs of sensor and IVC models. These models reduce the update frequency and introduce worst case real-world delays to the data [19], [20], given in Table I.

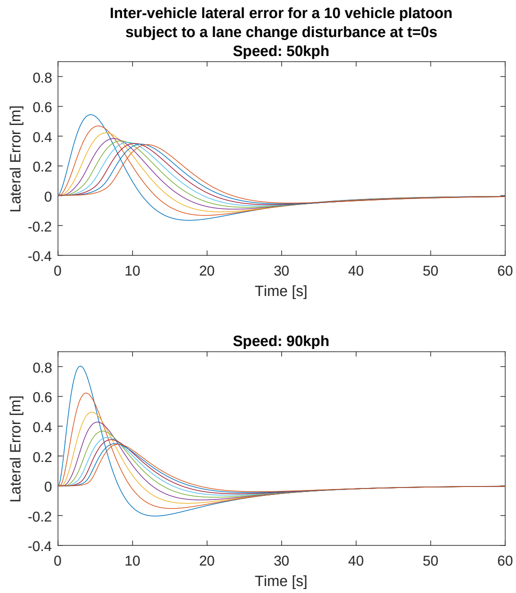

Fig. 8. Lateral error during lane change manoeuvre at 50 and 90kph

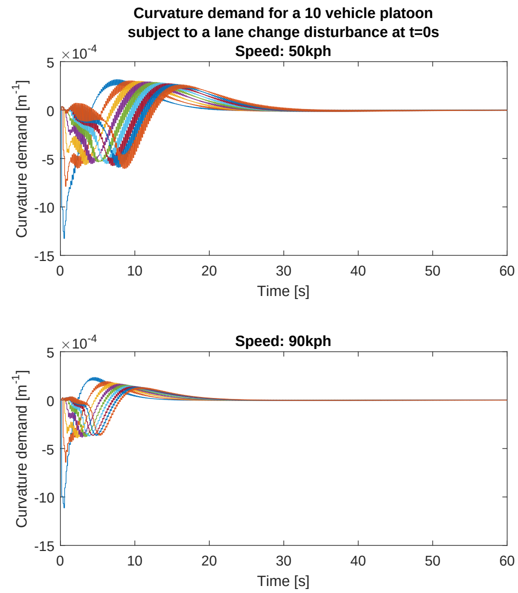

Fig. 9. Curvature demand during lane change manoeuvre at 50 and 90kph

B. Lane change manoeuvre

In order to test the performance and string stability of the lateral controller, a simulation of a lane change manoeuvre was performed, as illustrated in Fig. 6. The control parameters used during the test are shown in Table II. It is clear that these parameters meet the string stability criteria given by (21), and (25) yields a maximum permissible delay of $938ms$ which is acceptable.

1) Nominal conditions: Fig. 8 shows the inter-vehicle lateral error $(y_i - y_{i-1})$ in a 10 vehicle platoon (1 leader, 9 followers), subject to a lane change by the leader at $t = 0s$, at both $50kph$ and $90kph$. It can be seen that as the disturbance propagates through the platoon, the peak error experienced by subsequent vehicles reduces, confirming string stability. Fig. 9 illustrates the curvature demand produced by the control system during this manoeuvre.

2) During a steady state cornering: In addition to rejecting disturbances on a straight road, a platoon must also perform well during steady state cornering. For this test, two lane changes are performed at $50kph$, one in each direction, to determine if the direction of the corner has any effect on performance. The corner radius is $1000m$.

TABLE I
SENSOR AND V2V MODEL PARAMETERS

	Frequency $[Hz]$	Delay $[ms]$
Sensor	25	100
V2V	10	10

TABLE II
CONTROL PARAMETERS

Parameter	a	b	c	λ
Value	0.5	1	0.1	0.1

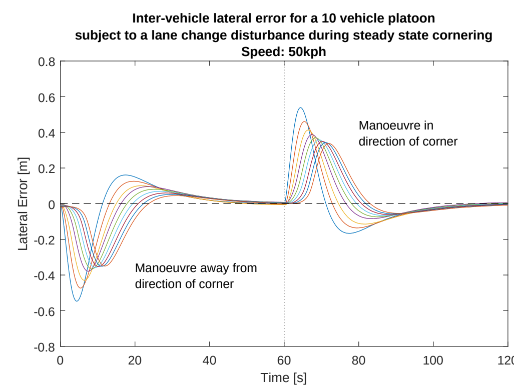

Fig. 10. Lateral error during lane change manoeuvres during steady state cornering

Fig. 10 illustrates the performance of the lateral controller during steady state cornering. It is clear that the direction of the manoeuvre has no noticeable effect on the controller performance and that string stability is maintained throughout.

3) Worst case delay: The tests above were subject to small sensor and communication delays, significantly below the limit imposed by (25). A final series of tests was conducted to investigate the performance of the controller as this limit is reached. Fig. 11 illustrates the inter-vehicle lateral position error damping ratio $(\Delta y_i / \Delta y_{i-1})$ along the platoon, with increasing sensor delay[1]. A damping ratio of less than unity for all vehicles in a given platoon confirms its string stability.

It can be seen that up to a sensor delay of $600ms$, nominal controller performance is maintained, but by $700ms$ the final vehicle is string unstable. As the delay is further increased this instability propagates forward through the platoon. In

[1]Only sensor/actuator delay was modelled in the derivation of (25), communications delay requires further investigation

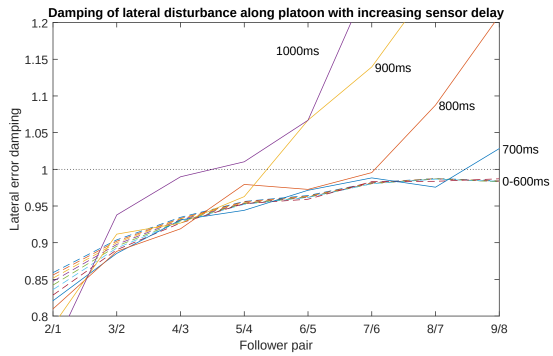

Fig. 11. String stability assessment with increasing sensor delay

addition to the $700ms$ sensor delay, there are additional sources of delay present in the high-fidelity simulation, such as

- Steering actuator lag ($\sim 50ms$)
- Discrete sampling of sensor data ($40ms$)
- Discrete sampling of communication data ($100ms$)
- Communications delay ($10ms$)

This leads to a total delay of $\sim 900ms$ being required in order to induce string instability, which is very close to predicted value of $938ms$ from (25). It is anticipated, however, that the actual delay is lower than the prediction due to the presence of additional sources of error not accounted for in the derivation of (25), such as those discussed in Sections II-D and II-E.

V. Conclusions & Further Work

This paper has derived a lateral controller for platooning vehicles which uses only information which can realistically be obtained, range and azimuth measurements between follower and preceding vehicles augmented by additional IVC information.

Based on this estimated lateral position, a controller has been developed which can guarantee string stability provided a maximum sensor delay is not exceeded. This controller has been shown to exhibit string stability in both the nominal case and in the presence of delays up to the maximum. To demonstrate the controller performance, high fidelity simulations were performed using MATLAB/Simulink interfaced with TORCS to provide a dynamic model. These simulations were conducted across a range of typical motorway operating speeds, during steady state cornering and were subject to realistic measurement and communication models. The simulation results illustrate stable and robust performance across all of these conditions, in addition to confirming the validity of the theoretical maximum permissible delay.

This paper has presented an initial assessment of the robustness of the controller to sensing and actuation delays. However, further work is needed to assess the impact of sensing and communication delays separately, in addition to determining the minimum required communication rates. This is necessary to inform the choice of sensors and IVC equipment to ensure they meet the minimum requirement for lateral platoon string stability under all operating conditions. A more detailed analysis of the controller robustness will also include an assessment of the sensitivity of the lateral position estimate to delays and sampling rates.

References

[1] D. Flatley, L. Reyner, and J. A. Horne, "Sleep-related crashes on sections of different road types in the uk (1995-2001)," *ROAD SAFETY RESEARCH REPORT 52*, 2004.

[2] R. Rajamani, H.-S. Tan, B. K. Law, and W.-B. Zhang, "Demonstration of integrated longitudinal and lateral control for the operation of automated vehicles in platoons," *Control Systems Technology, IEEE Transactions on*, vol. 8, no. 4, pp. 695–708, 2000.

[3] P. Seiler, A. Pant, and K. Hedrick, "Disturbance propagation in vehicle strings," *Automatic Control, IEEE Transactions on*, vol. 49, no. 10, pp. 1835–1842, 2004.

[4] E. Chan, P. Gilhead, P. Jelínek, P. Krejci, and T. Robinson, "Cooperative control of sartre automated platoon vehicles," in *Proceedings of the 19th ITS World Congress*, 2012.

[5] Y. Zhao, P. Minero, and V. Gupta, "On disturbance propagation in leader–follower systems with limited leader information," *Automatica*, vol. 50, no. 2, pp. 591–598, 2014.

[6] G. Guo and W. Yue, "Sampled-data cooperative adaptive cruise control of vehicles with sensor failures," *Intelligent Transportation Systems, IEEE Transactions on*, vol. 15, no. 6, pp. 2404–2418, 2014.

[7] A. Davila, "Report on fuel consumption," SARTRE, Tech. Rep., 2013.

[8] G. Lee, S. Kim, Y. Yim, J. Jung, S. Oh, and B. Kim, "Longitudinal and lateral control system development for a platoon of vehicles," in *Intelligent Transportation Systems, 1999. Proceedings. 1999 IEEE/IEEJ/JSAI International Conference on*. IEEE, 1999, pp. 605–610.

[9] A. Davila, "Report on infrastructure and environment," SARTRE, Tech. Rep., 2012.

[10] J. W. Lee, "A machine vision system for lane-departure detection," *Computer vision and image understanding*, vol. 86, no. 1, pp. 52–78, 2002.

[11] M. L. Sichitiu and M. Kihl, "Inter-vehicle communication systems: a survey," *Communications Surveys & Tutorials, IEEE*, vol. 10, no. 2, pp. 88–105, 2008.

[12] D. Swaroop, "String stability of interconnected systems: An application to platooning in automated highway systems," *California Partners for Advanced Transit and Highways (PATH)*, 1997.

[13] L. Papadimitriou, G. Lu, and M. Tomizuka, "Autonomous lateral following consideration for vehicle platoons," in *Advanced Intelligent Mechatronics, 2003. AIM 2003. Proceedings. 2003 IEEE/ASME International Conference on*, vol. 1. IEEE, 2003, pp. 401–406.

[14] S. Solyom, A. Idelchi, and B. B. Salamah, "Lateral control of vehicle platoons," in *Systems, Man, and Cybernetics (SMC), 2013 IEEE International Conference on*. IEEE, 2013, pp. 4561–4565.

[15] J. Ackermann, J. Guldner, W. Sienel, R. Steinhauser, and V. I. Utkin, "Linear and nonlinear controller design for robust automatic steering," *Control Systems Technology, IEEE Transactions on*, vol. 3, no. 1, pp. 132–143, 1995.

[16] R. Rajamani, *Vehicle dynamics and control*. Springer, 2011.

[17] B. Wymann, E. Espié, C. Guionneau, C. Dimitrakakis, R. Coulom, and A. Sumner, "TORCS, The Open Racing Car Simulator," http://www.torcs.org, 2014.

[18] O. McAree, "TORCSLink: First release," Jan 2015. [Online]. Available: http://dx.doi.org/10.5281/zenodo.13943

[19] R. Rajamani and S. Shladover, "An experimental comparative study of autonomous and co-operative vehicle-follower control systems," *Transportation Research Part C: Emerging Technologies*, vol. 9, no. 1, pp. 15–31, 2001.

[20] M. Xiaomin, C. Xianbo, R. Hazem H *et al.*, "Performance and reliability of dsrc vehicular safety communication: a formal analysis," *EURASIP Journal on Wireless Communications and Networking*, vol. 2009, 2009.